

## Pulsed laser vaporization and deposition

P. R. Willmott\* and J. R. Huber

*Physikalisch-Chemisches Institut der Universität Zürich, Winterthurerstrasse 190,  
CH-8057 Zürich, Switzerland*

Photons have many advantages for vaporizing condensed systems, and laser vaporization sources have a flexibility not available with other methods. These sources are applied to making thin films in the well-known technique of pulsed laser deposition (PLD). The vaporized material may be further processed through a pulsed secondary gas, lending the source additional degrees of freedom. Such pulsed-gas sources have long been exploited for fundamental studies, and they are very promising for film deposition, as an alternative to chemical vapor deposition or molecular beam epitaxy. The authors outline the fundamental physics involved and go on to discuss recent experimental findings.

### CONTENTS

I. Introduction	315
II. Pulsed Laser Deposition	317
A. General features	317
B. Light-material interaction	318
C. Plasma generation	318
D. Macroscopic particulate production	320
E. Plasma expansion and recondensation	320
F. Film growth	321
G. Femtosecond ablation	322
III. Pulsed Reactive Crossed-Beam Laser Ablation	322
A. Principal features	322
B. Reactive scattering processes	323
IV. Concluding Remarks	327
Acknowledgments	327
References	327

### I. INTRODUCTION

One of the principal challenges in solid-state physics today is the discovery and application of novel materials and their incorporation in solid-state devices for use in areas as diverse as biophysics, optoelectronics, and nanotechnology. As size continues to fall below micron dimensions, and heterogeneous materials are integrated in a single device, it becomes paramount to understand the fundamental processes and microscopic mechanisms at play in order to control film deposition.

Incorporation of novel materials in, for example, standard silicon technology presents problems of crystallographic incommensurability and incompatible thermodynamic properties. Established thermal growth techniques may be unable to accommodate two chemical systems on the same substrate: for example, the growth conditions needed for one can result in the thermal decomposition of the other. The ability to deposit films under nonthermal conditions may alleviate such difficulties.

The regime of nonthermal interactions in its most general sense describes physical and chemical processes such as the breaking and making of chemical bonds by ensembles of species that have energy distributions that cannot be described by the Maxwell-Boltzmann equation and therefore cannot be described by a single temperature. Such distributions are said to deviate from thermal equilibrium and might be achieved if energy can be selectively and nonthermally pumped (for example, by laser light or an electric field) into one degree of freedom that is effectively decoupled from the rest of the molecular or atomic system. In practice, this becomes interesting if reaction activation barriers can be transcended or indeed lowered by nonthermally manipulating the electron energy distribution (the electrons have negligible thermal mass) while maintaining a low “temperature” for the rest of the system, which carries the vast majority of the thermal mass. Hence, in electrical discharge growth techniques, the process chamber remains cool although the “temperature” of the electrons may be many thousands of degrees Kelvin.

Soon after their introduction in 1962, it was recognized that high-powered pulsed lasers could be used as a flexible and powerful tool for studying the interaction of intense electromagnetic fields with solid material (Frichenicht, 1973). The dominant mechanisms involved in such processes and in the resulting formation of a hot plasma from the irradiated surface were found to depend sensitively on laser parameters such as the energy density (fluence), pulse duration, wavelength, polarization, laser repetition rate, as well as the material being irradiated. Theoretical models describing light-material interaction and the subsequent liberation of gas-phase species have become increasingly sophisticated as more experimental data have become available (Geohegan, 1992; Kelly *et al.*, 1992; Sibold and Urbassek, 1992; Kelly and Miotello, 1993). A general feature of ablation plasmas (also known as “plumes”) is their high ion and electron temperatures of the order of several thousand Kelvin, and their high degree of ionization (von Engel, 1965).

\*Electronic address: willmott@pci.unizh.ch

One of the most important applications of the interaction of high-powered laser light with condensed material is pulsed laser deposition (PLD). It has become increasingly popular within research laboratories as a method of producing thin films of novel materials ever since laser pulses in the nanosecond (ns) regime became available in the late 1970s and even more so since its success in the growth of commercial cuprate superconductor thin-film devices in the late 1980s. Despite this, PLD has still to fulfill its commercial promise, particularly in semiconductor applications, in which the necessity of device grade purity and high crystallographic perfection has proved to be the major stumbling block.

We now set out the general physical requirements that must be satisfied by thin-film production techniques, ignoring technical obstacles such as vacuum purity. We restrict our discussion to the fabrication of high quality epitaxial thin films for electronic and optical applications, for which demands on crystalline perfection are most stringent.

After an atom or ion is adsorbed on a surface, it might diffuse across the surface and then escape once more to the vacuum, or it might become bonded as an adatom (Lewis and Anderson, 1978; Venables *et al.*, 1984). The diffusion rate of an adatom across a surface is given by

$$D_s = D_0 \exp\{-\varepsilon_D/kT\}, \quad (1)$$

where  $\varepsilon_D$  is the activation energy for diffusion and is typically around 2–3 eV on an atomically flat covalent surface, but depends strongly on the nature of the adsorption and on the local environment in which the atom finds itself. In any case, there must be sufficient surface diffusion to allow adatoms to migrate to thermodynamically stable sites and minimize their surface energy within the time needed to deposit a monolayer of atoms.

A potential problem with enhancement of surface diffusion by increasing the surface temperature is the concomitant increase in surface-to-bulk diffusion and bulk interdiffusion. This leads to a smearing out of boundary planes and a consequent lower limit to device size. Instead of increasing the temperature, a possible solution is to enhance surface mobility by energy transfer from species impinging from the gas phase to surface species. The question then arises as to the optimal energy transfer needed to promote surface mobility while avoiding bulk displacement phenomena.

In their theoretical study of ion-induced surface and bulk displacements, Brice *et al.* (1989) developed a simple molecular-dynamics model in which the displacement of atoms in the uppermost monolayer was possible when bombarded with homonuclear species with energies as low as half the bulk displacement energy, whereas the incident energy needed to displace atoms in the second monolayer or deeper somewhat exceeded the bulk displacement energy due to energy loss in traversing the surface layer. So, for Si on Si, the model predicted enhanced surface mobility via ion-induced displacement without damage to the bulk if incident energies ranged between 11 and 38 eV. Increasing the energy to 100 eV resulted in one bulk displacement (i.e.,

defect) for every two surface displacements. Experimental data have shown agreement within a factor of 2 with this model (Burger and Reif, 1987; Nagai *et al.*, 1988). Enhanced surface mobility caused by bombardment therefore allows the experimenter to deposit at lower temperatures. Sankur *et al.* (1989) showed, for example, that Ge heteroepitaxy was possible at 300 °C using PLD, while for molecular-beam epitaxy (MBE), temperatures in excess of 700 °C are required.

Finally, we address the problem of stoichiometric growth in compound films. Particularly for compound semiconductors, the specifications for stoichiometry far exceed the accuracy with which the ratio of fluxes can be controlled. In general, the experimenter turns to Le Chatelier's principle (equilibrium chemistry) to ensure that any excess material remains in the gas phase and can be pumped away. This is achieved by careful choice of deposition parameters such as temperature and partial pressures, which will in turn affect the rate of reaction. The use of nonthermal chemistry opens up the possibility to work far from chemical equilibrium and select more favorable deposition conditions.

It is outside the scope of this colloquium to provide a treatise of all research and commercial growth methods, for which the reader is referred to Hirvonen (1991), Bunshah (1994), and Hubler (1994). It is, however, useful to outline the most common methods to provide a standard for comparison with PLD.

We define thermal deposition techniques as those in which the kinetic energies of the impinging particles is of the order of 0.1 eV. Conceptually, the most simple approach to transport material from the bulk onto a thin film is via thermal evaporation. This technique was indeed the first method to be employed for film growth and is still used today in a refined manner in the form of molecular-beam epitaxy.

In chemical vapor deposition (CVD) and metalorganic chemical vapor deposition (MOCVD), transport to the growing film is facilitated by using volatile compounds of the element of interest. These precursors are introduced into a vacuum chamber at pressures typically of the order of 10 Pa where they are allowed to decompose thermally or react on or above a heated substrate. The element of interest is chemisorbed on the surface while the decomposition fragments remain volatile and are pumped away. Incorporation of some of the volatile decomposition fragments in the growing film can degrade its quality, which can be particularly problematic in MOCVD with carbon and oxygen, though even hydrogen incorporation from decomposition from hydrides has been famously shown in GaN production to seriously affect its electronic properties (Nakamura *et al.*, 1992). CVD and MOCVD dominate large scale commercial production of electronic materials, due to their high and spatially homogeneous growth rates, subsequent modest vacuum requirements, and low cost.

Thermal techniques suffer from the limitation that each degree of freedom in the partition function of a participating chemical system has the same temperature. It may be advantageous if one particular energetic de-

gree of freedom could be nonthermally accessed, thereby shifting a chemical reaction away from thermal equilibrium. This is commonly achieved in film growth by, for example, use of an electric discharge plasma in plasma-enhanced CVD.

Ion-beam techniques are nonthermal methods in which the energy of the impinging flux can be controlled by an electric field. A promising technique is sputtering (Bunshah, 1994). Although differing in detail, all sputtering techniques extract positive ions from an electrical discharge (usually  $\text{Ar}^+$ ) and accelerate them onto a target. The target is therefore eroded or “sputtered” and a beam of target atoms with energies between 10 and 100 eV is produced. Sputtering suffers, however, from problems of impurities mainly because (a) a pressure range from about 1 to 100 Pa of working gas is needed to ignite the electrical discharge, and (b) the sputtering plasma also erodes surfaces other than the intended target.

The motivation for using any given deposition technique is driven by the balance of its strengths and weaknesses: CVD is favored for the industrial production of Si-based integrated circuits where typical dimensions are several microns and high throughput is at a premium, while MBE is preferred for quantum well devices where film growth must be controlled at a subnanometer level and high crystal purity is essential. Nonthermal methods such as sputtering have proved to be advantageous for congruent (i.e., where the elemental ratios in the original material are preserved in the deposited film) transfer of multielemental materials which, if thermally heated, would decompose before a sufficient vapor pressure was reached.

In the next section, we describe the fundamental processes that occur in the ablation and deposition of materials. This prepares us for Sec. III, in which we describe the new features that are brought in by a pulsed secondary gas. The resulting pulsed reactive crossed-beam ablation, known already as a research tool, appears to be very promising technologically.

## II. PULSED LASER DEPOSITION

Pulsed laser deposition (PLD) is a growth technique in which photonic energy is coupled to the bulk starting material via electronic processes. The principle of PLD is shown in Fig. 1. An intense laser pulse passes through an optical window of a vacuum chamber and is focused onto a solid or liquid surface (the “target”), where it is partially absorbed. Above a certain power density, significant material removal occurs in the form of an ejected luminous plume. The threshold power density needed to produce such a plume depends on the target material, its morphology, and the laser pulse wavelength and duration, but might be of the order of  $10\text{--}500\text{ MW cm}^{-2}$  for ablation using ultraviolet (UV) excimer laser pulses of 10 ns duration. Material from the plume is then allowed to recondense on a substrate, where film growth occurs. The growth process may be supplemented by a passive or reactive gas or ion source, which may affect

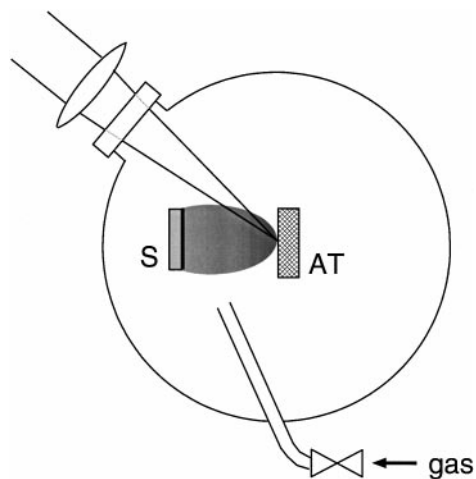


FIG. 1. The principle of pulsed laser deposition (PLD). A high intensity laser pulse is focused onto an ablation target (AT) in a vacuum chamber. The surface region is vaporized where the laser spot impinges on it. The partially ionized liberated material, or “ablation plume” is then allowed to settle and form a thin film on a substrate S positioned downstream. Growth may be modified by provision of a reactive gas.

the ablation plume species in the gas phase or the surface reaction, in which case one talks of reactive PLD.

### A. General features

The physical processes in PLD are highly complex and interrelated, and depend on the laser pulse parameters and the properties of the target material. We want to convey the most important physical phenomena in PLD and limit ourselves here to general features, including the coupling of electromagnetic radiation with condensed matter, the subsequent production of a nascent plasma, and finally its expansion away from the target and recondensation on a substrate. As far as is possible, we remain material unspecific. For more detailed aspects of PLD, see Chrisey and Hubler (1994).

Laser ablation for thin film growth has many advantages: (i) the energy source (laser) is outside the vacuum chamber which, in contrast to vacuum-installed devices, provides a much greater degree of flexibility in materials use and geometrical arrangements; (ii) almost any condensed matter material can be ablated; (iii) the pulsed nature of PLD means that film growth rates may be controlled to any desired amount; (iv) the amount of evaporated source material is localized only to that area defined by the laser focus; (v) under optimal conditions, the ratios of the elemental components of the bulk and film are the same, even for chemically complex systems; (vi) the kinetic energies of the ablated species lie mainly in a range that promotes surface mobility while avoiding bulk displacements; (vii) the ability to produce species with electronic states far from chemical equilibrium opens up the potential to produce novel or metastable materials that would be unattainable under thermal conditions. PLD also has technical and fundamental drawbacks, in particular: (i) the production of macroscopic

ejecta during the ablation process; (ii) impurities in the target material; (iii) crystallographic defects in the film caused by bombardment by high kinetic energy ablation particles; (iv) inhomogeneous flux and angular energy distributions within the ablation plume.

Some of these problems present surmountable engineering challenges (within economic constraints), while others appear more fundamental. We discuss these advantages and disadvantages as they naturally arise in the description of the physical processes below.

## B. Light-material interaction

When laser radiation is absorbed in the surface region of a condensed-matter target, the electromagnetic energy is immediately converted into electronic excitation in the form of plasmons, unbound electrons and, in the case of insulators, excitons. The response is described by the dielectric function  $\epsilon(\omega, K)$  and depends sensitively on the electronic band structure. How the light is absorbed depends on the processes at play. The electric-field amplitude  $E$  of an electromagnetic wave is given by

$$E = \left( \frac{2\Phi}{cn\epsilon_0} \right)^{1/2}, \quad (2)$$

where  $\Phi$  is the power density,  $\epsilon_0$  is the permittivity of free space,  $c$  is the velocity of light, and  $n$  is the refractive index. A material with a refractive index of 2 containing radiation of  $2 \times 10^8 \text{ W cm}^{-2}$  power density will therefore be subjected to a field strength of  $2 \times 10^5 \text{ V cm}^{-1}$ , sufficient to cause dielectric breakdown in many materials. The threshold electric-field strength for dielectric breakdown is therefore proportional to the square root of the power density, which in turn is proportional to the laser fluence and inversely proportional to the laser pulse duration  $\tau$ .

In most cases, however, material removal is controlled by the rate of thermal conduction through the lattice, which according to Fick's law of diffusion means that the threshold fluence is proportional to  $\sqrt{\tau}$ . Above  $\tau \sim 20 \text{ ps}$ , ablation therefore occurs via conventional heat deposition. The physical processes governing for time scales below that for electron-lattice coupling of  $\sim 10 \text{ ps}$ , where heat diffusion can no longer play a role, are discussed separately in Sec. II.G. The excited electrons transfer their energy to the lattice within a few picoseconds and heating begins within the optical absorption depth of the material  $1/\alpha$ , where  $\alpha$  is the optical absorption coefficient. If the thermal diffusion length, given by  $l_T = 2\sqrt{D\tau}$ , where  $D$  is the thermal diffusion constant, is smaller than  $1/\alpha$ , the bulk will be heated down to  $1/\alpha$ , independent of pulse duration. In ablation of multielemental targets, congruent evaporation can only be guaranteed if this condition is met, hence the use of fast UV laser sources is favored. This unique capacity of PLD has recently been elegantly illustrated in its use in growing Nd- and Cr-doped gadolinium scandium gallium garnet (Nd,Cr:GSGG) heteroepitaxially on Si(001).

Nd,Cr:GSGG contains six different elements and 160 atoms in a unit cell (Willmott *et al.*, 1999a)

The ablation of metals represents the opposite extreme in which the absorption depths are typically of the order of 10 nm, while the thermal diffusion lengths only become this small when using femtosecond pulses. A simple interpretation of this would be to assume that when  $1/\alpha \ll l_T$ , all the photonic energy is deposited into the absorption layer, and is efficiently thermally transported during the laser pulse to a depth of  $l_T$ . This would result in the effusion of thermal particles of typically 0.25 eV as the vaporization front moves with a velocity of  $l_T/\tau$  to a depth of  $l_T$ . For ns ablation, the situation is, however, complicated by ionization of the nascent erosion cloud before the laser pulse is over. Transfer of energy from the electrons to the lattice occurs within a few picoseconds, and heating of the absorption layer will begin. For example, the extinction coefficient of Ti at  $\lambda = 248 \text{ nm}$  (KrF excimer radiation) is  $k = 1.21$ , and its reflectivity is 0.236. The absorption depth is therefore  $\lambda/(4\pi k) = 16 \text{ nm}$ . If we assume a focus spot on the target of  $1 \text{ mm}^2$ , the absorption volume contains approximately  $10^{-9}$  mole. The molar enthalpy of vaporization of Ti is  $421 \text{ kJ mol}^{-1}$ , hence about  $400 \mu\text{J}$  is required to raise this volume to the vaporization temperature of  $\approx 3600 \text{ K}$ . If the total photonic energy in the laser pulse is around 100 mJ, vaporization of the absorption depth will begin after about the first 100 ps of a 20-ns pulse. Thereafter, the bulk material under the plasma is largely screened from the remainder of the laser pulse, which is efficiently absorbed by the plasma as it becomes increasingly ionized. This process is known as laser supported absorption and will produce plasma species with high kinetic energies ranging between 1 eV and more than 100 eV (Wiedeman and Helvajian, 1991; Dreyfus, 1991). Laser supported absorption generates the hottest species and lowest ablation yields for bulk materials with a high value of  $\alpha$ . It is these highly energetic plasma species that provide the possibility of surface processes far from thermal equilibrium.

When laser supported absorption becomes dominant, the effective thermal diffusion length is reduced to  $l_T^{\text{eff}} = 2\sqrt{D\tau_{\text{eff}}}$  where  $\tau_{\text{eff}}$  is the time needed to create an erosion plasma after the start of the laser pulse. For the example above,  $l_T^{\text{eff}}$  is some tens of nm, which is indeed a typical average depth of an erosion crater produced by a nm pulse on metallic surfaces (Timm *et al.*, 1996).

## C. Plasma generation

What are the physical processes at play in laser supported absorption? After a ns laser pulse, the degree of ionization of the plasma is for most materials close to unity. The mechanisms responsible for generating such a high degree of ionization remain contentious. It has been mooted that laser supported absorption occurs by inverse bremsstrahlung. We now develop a simple physical model to determine the conditions for which inverse bremsstrahlung might plausibly be thought responsible for igniting and ionizing a nascent plasma. We will see

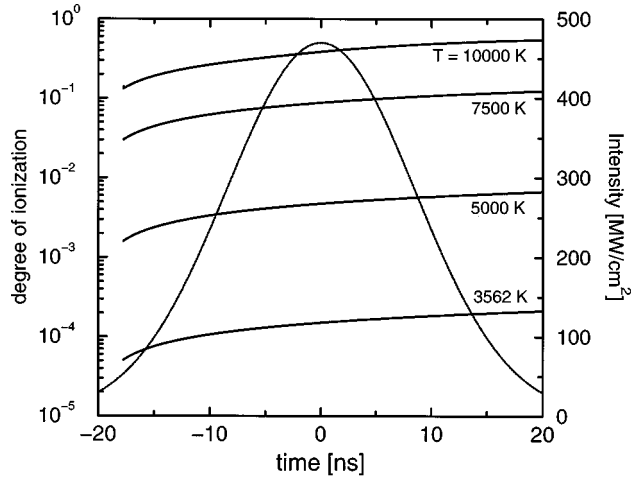


FIG. 2. Evolution of the degree of ionization of a nascent Ti erosion cloud by inverse bremsstrahlung during irradiation with a  $10 \text{ J cm}^{-2}$ , 20-ns laser pulse at 248 nm for different initial plasma temperatures, calculated using the Saha equation, Eq. (3). The left logarithmic scale is for the degree of ionization, while the right linear scale shows the laser-pulse power density.

that although unrealistically high initial plasma temperatures have to be assumed to achieve a high degree of ionization with typical UV ns-laser pulses, the intrinsic instability of inverse bremsstrahlung (which means that local deviations from the average are rapidly amplified) can account for the experimental findings.

We begin at  $t = t_{\text{vap}}$ , just as sufficient photonic energy has been deposited into the optical absorption depth to cause its evaporation. For a gas at local thermal equilibrium, the density of singly charged ions  $n_i$  in  $\text{cm}^{-3}$  is given by the Saha equation

$$n_i = (2.4 \times 10^{15} T^{3/2} n_n e^{-U_i/kT})^{1/2}, \quad (3)$$

where  $T$  is the gas temperature in K,  $n_n$  is the density of neutrals in  $\text{cm}^{-3}$ , and  $U_i$  is the first ionization potential of the gas atoms in question in electron volts (Chen, 1974). We take the starting temperature as the vaporization temperature  $T_{\text{vap}}$ . The absorptivity by inverse-bremsstrahlung of this cloud to radiation of frequency  $\nu$  (in Hz) is given by (Hughes, 1975)

$$\alpha_{\text{IB}} = 3.7 \times 10^8 \frac{Z^3 n_i^2}{T^{1/2} \nu^3} (1 - e^{-h\nu/kT}), \quad (4)$$

where  $Z=1$  is the elemental charge of the ion,  $n_i$  is in  $\text{cm}^{-3}$ , and  $\alpha_{\text{IB}}$  is given in  $\text{cm}^{-1}$ . As the cloud absorbs via inverse bremsstrahlung, it will become hotter, more ionized, and in turn absorb more efficiently.

We show the evolution of the plasma using this model for Ti in Fig. 2 from  $t_{\text{vap}}$  until the end of the laser pulse, assuming that the plasma propagates in the  $z$  direction normal to the target surface, and its cross section  $A$  remains constant. The laser pulse is a 20-ns Gaussian with a total fluence of  $10 \text{ J cm}^{-2}$ . For a cloud having an

initial temperature  $T = T_{\text{vap}} = 3562 \text{ K}$ , the degree of ionization after the laser pulse is seen to remain under  $10^{-3}$ .

The degree of ionization immediately after the laser pulse is extinguished has, however, been found experimentally to be between 0.1 and 1, although this is then thought to fall off rapidly by electron recombination further downstream (see below). In order to obtain such a high degree of ionization, we would have to assume a starting temperature of  $\sim 10000 \text{ K}$  which appears unreasonable. Therefore only nonthermal desorption and ionization processes can generate locally high concentrations of electrons in the nascent ablation cloud starting at  $T_{\text{vap}}$ . Local nonuniformities in electron density in volumes of dimensions comparable to the mean free path of the electrons  $\lambda_e \sim 1 \mu\text{m}$ , thought to be caused by laser focus ‘‘hot spots,’’ multiphoton ionization, surface impurities, and statistical variations, can seed a runaway breakdown of the entire ablation cloud by inverse bremsstrahlung on the time scale of femtoseconds. The probability of this occurring depends on the photon energy and flux, but may in many cases be inevitable when one considers that  $\lambda_e^3$  is some  $10^5$  times smaller than the volume of the nascent erosion cloud (Dreyfus, 1991, Wiedeman and Helvajian, 1991).

Although the bulk behind the nascent plasma is shielded from further direct ablation, it is certainly affected by the plasma itself. Immediately after the laser pulse is extinguished, initial temperatures within the still localized plasma can be in excess of 20000 K. The plasma thickness is still a small fraction of a millimeter after ablation with a ns pulse. Using typical ablation yields for metals of  $10^{15}$  particles per pulse, Boyle’s law predicts pressures of up to  $10^9 \text{ Pa}$ , and such values have indeed been reported (Ready, 1978; Russo, 1995; Chang and Warner, 1996). In general, the initial plasma pressure will be highest for those materials with high bulk optical absorption for the same reasons as given above.

Some of the internal energy of the nascent plasma will be thermally coupled to the target material while it remains in close contact, which may cause a transient localized melt to a depth of  $\sim 1 \mu\text{m}$  and further vaporization at the laser focus. Indeed, for the ablation of metals, most of the photonic energy is ultimately coupled to the target bulk. For a typical ablation event where a 100-mJ ns-pulse removes  $10^{15}$  atoms, only 10% of the input energy is accounted for even if we assume that every particle has emitted a 5-eV photon, is singly ionized, and recoils with a kinetic energy of 50 eV (Svendsen *et al.*, 1996; Timm *et al.*, 1996). Experiments by our group on Ti metal, in which 50000 laser shots of 100 mJ each, resulted in the 60-g target rod to be 50 K above room temperature immediately after removal from the chamber. Even if no thermal radiation loss had occurred, this temperature increase requires nearly 1600 J or a third of the experiment’s total photonic input energy (Timm *et al.*, 1996).

The energy coupled to the target bulk is hence both thermal and mechanical and can have detrimental effects on film growth due to the ejection of macroscopic particulates.

#### D. Macroscopic particulate production

The bulk metal in intimate contact with the nascent plasma will suffer a recoil with forces of up to  $10^4$  N during the laser irradiation. We have seen in our experiments of ablation of liquid Al and Ga (see below) that the 1-cm-diameter liquid balls shake with amplitudes estimated at some tenths of a millimeter after each laser shot. The mechanical forces on a target can lead to the ejection of macroscopic particulates generically labeled “laser droplets.”

The production of laser droplets perhaps represents the greatest obstacle to the use of PLD in commercial applications. Their occurrence results from three phenomena, namely subsurface boiling, recoil ejection, and exfoliation. The first two of these are termed “splashing” phenomena and, to a first approximation, are independent of the target morphology and can produce droplets from a single laser shot. Subsurface boiling will occur in materials in which the time needed to convert laser energy into heat and transfer it into the bulk is shorter than the time needed to evaporate the surface layer, defined as having a thickness of the order of the skin depth (Ready, 1963),

$$\delta = (2/\mu_0 \sigma \omega)^{1/2}, \quad (5)$$

where  $\mu_0$  is the permittivity of free space,  $\sigma$  is the electrical conductivity, and  $\omega$  is the angular frequency of the incoming light. This explosive phase transition, which produces micron-sized droplets, is negligible in dielectric materials as  $\sigma$  is so small, though in metals with low melting temperatures and high thermal conductivities (e.g., Al,  $\delta_{248\text{ nm}} \approx 2.3\ \mu\text{m}$ ), this process may be dominant, and can only be suppressed by using sufficiently low laser fluences, with the attendant reduction in the ablation yield.

When the transient melt below the laser focus spot is subjected to the recoil pressure exerted by the expanding plume, droplets can be ejected as the melt is squeezed onto the solid bulk. As the typical size of droplets in recoil ejection is similar to that in subsurface boiling, it is hard to distinguish between them, though the angular distribution in recoil ejection has more of a crown form than that in subsurface boiling, which shows a  $\cos^n \theta$  dependence.

The final hydrodynamic effect is termed “exfoliation” and describes particulate ejection due to increased surface roughening by repeated melt-freeze cycles of the irradiated material. Eventually, the macroscopic outgrowths become necked off and thermally decoupled, and break away as particulates. These may have dimensions of many microns, depending on the material. Because exfoliation is a morphological process that requires two or more laser shots, it may be avoided by careful target surface preparation and refreshment. This can be achieved either by repositioning the target or laser focus before surface roughening becomes critical (Timm *et al.*, 1996) or by using liquid targets (Sankur *et al.*, 1989; Xiao *et al.*, 1996; Willmott and Antoni, 1998).

#### E. Plasma expansion and recondensation

We now turn to the expansion of the nascent erosion plasma into vacuum or an ambient gas. Fluid dynamic models have been successfully applied to the expanding erosion cloud by many groups (Kelly *et al.*, 1992; Sibold and Urbassek, 1992; Kelly and Miotello, 1993). When the ablation yield is much above about 0.1 monolayers per nanosecond, as is normally the case in PLD, the particles cannot escape collisionlessly and there will be a layer in contact with the target in which reflections and collisions occur which will tend to thermally equilibrate the plasma and lower its degree of ionization. This so-called Knudsen layer modifies the distribution to a drifted Maxwellian with a center-of-mass velocity  $\bar{v}$  normal to the surface given by

$$P(v) \sim v^3 \exp\{-m(v - \bar{v})^2/2kT\}. \quad (6)$$

A knowledge of the degree of ionization of the ablation plasma as it impinges on a growing surface is vital, as it is here, where the substrate acts as a third body and energy sink that most of the chemistry occurs. The degree of ionization depends on the laser wavelength, pulse duration, fluence, and target material, and will also change as the plasma expands. That there is a significant amount of neutrals present is substantiated by there being a *visible* glow—luminescent relaxation of electronically excited positive ions results primarily in UV photons. Optical spectroscopy is a powerful method for measuring the temporal and spatial distribution of ions and neutrals and their relative abundance in the plume (Archbold *et al.*, 1964; Hendron *et al.*, 1996). Efforts have been made to extract the degree of ionization using Langmuir or ion probes (Segall and Koopman, 1973; Hansen *et al.*, 1997; Willmott *et al.*, 1997). There are several potential systematic errors associated with this technique, including plasma sheath distortion due to charge buildup, local electric field inhomogeneities, and chemical modification of the probe surface (Chapman, 1980; Hendron *et al.*, 1996). Interpretation of the data must therefore be approached with caution (Hansen *et al.*, 1997).

Time-of-flight mass spectroscopy (TOFMS) and time-of-flight quadrupole mass spectroscopy (TOFQMS) are powerful and flexible analytical methods for identifying ablation species and their kinetic energies and do not rely on photoemission for detection: in species where internal conversion is efficient and the luminescence yield is low, such as in many clusters, mass spectroscopy has been shown to be invaluable (Curl and Smalley, 1991). Care must be exercised, however, as ablation plumes contain not only stable neutrals and possibly clusters, but also metastable species such as Rydberg atoms, ionic species, and electrons. In order to differentiate between these species, the experimental configuration must be chosen carefully (van Ingen, 1996; Willmott *et al.*, 1997).

Ion-electron recombination and electron transfer between ions and neutrals can occur while the particle densities are still high, which explains the existence of fast

neutrals in the plasma, and the generally lower degree of ionization once the plasma has become collisionless, typically after a few mm. When the initial degree of ionization is high (see above) the subsequent fraction of fast neutrals in the free expanding plume will also be high. Our group and that of Murray and Peeler (1993) have shown two contrasting cases. In UV nanosecond ablation of Ti the neutral species have kinetic energies typically about half those of the ions, due to efficient ion-electron recombination (Willmott *et al.*, 1997), while for 248-nm-ns ablation of carbon, in which the absorption depth is larger and hence the laser supported absorption is smaller, the kinetic energies of the neutrals were shown to be more than an order of magnitude lower than that of the ions (Murray and Peeler, 1993). When IR radiation was used (1064 nm) for ablation of carbon in experiments by Park and Moon (1998), inverse bremsstrahlung in the nascent plume was more efficient [Eq. (4)] and the neutrals had kinetic energies about one quarter of those for the ions.

As the plasma expands, it adiabatically cools to temperatures typically of 3000–5000 K (Geohegan, 1993), and the plasma species can have kinetic energies in a range as large as 1–500 eV, depending on the material, but is normally about 5–50 eV. The angular distribution of the plume has been fitted by many authors to a  $\cos^n \theta$  function, with values of  $n$  ranging from 2 to more than 20 (Weaver and Lewis, 1996). In general,  $n$  depends strongly on the laser fluence, and is lower when the plasma propagates into an ambient that is dense enough for there to be multiple collisions, which will broaden the angular distribution. The situation may be further complicated by intensity “wings” caused by shock fronts and, in the case of multicomponent targets, each element may have a different angular dependence. This beamlike distribution is often cited as a weakness in PLD in contrast to other techniques, limiting the deposition area typically to a few  $\text{cm}^2$ . Schey *et al.* (1998) demonstrated, however, that this can be advantageous if the position of the substrate is repeatedly rastered across the path of the ablation plume. Not only can large areas be homogeneously deposited, but most of the chamber remains free from long-term buildup of deposition material.

## F. Film growth

The diversity of thin films grown using PLD is enormous and perhaps recommends its flexibility more persuasively than anything else. It is outside the scope of this colloquium to list all the materials grown with PLD. Suffice it to say that the entire spectrum from transparent dielectrics, semiconductors, metals, to superconductors have all been successfully grown. The reader is recommended the bibliography by Saenger (1994) for a comprehensive list up to 1994. In the intervening five years, the catalogue has burgeoned still further.

The rationale for using PLD in preference to other deposition techniques lies primarily in its pulsed nature, the possibility of carrying out surface chemistry far from

thermal equilibrium, and, under favorable conditions, the ability to reproduce in thin films the same elemental ratios of even highly chemically complex bulk ablation targets. In Sec. I, we reasoned that there is a range of kinetic energies for the impinging species for which surface mobility and reactivity are enhanced while the bulk remains unaffected. The upper limit to this range depends on the bond strengths, but generally lies at about 50 eV. The kinetic energies of neutral species in a typical ns ablation plume normally lie well below the threshold for bulk damage, and, if necessary, it is normally possible to bias the substrate potential and so tune the ion energies appropriately.

Film growth and chemistry may be enhanced or modified by carrying out PLD in an ambient background gas. Gases are often used either to thermalize the plasma species through multiple collisions, or to compensate for the loss of an elemental component of the target through incongruent ablation (Gupta and Hussey, 1991). Reactive PLD, on the other hand, uses gases such as  $\text{H}_2$ ,  $\text{CH}_4$ ,  $\text{N}_2$ , or  $\text{O}_2$  to induce associative reactions primarily with metallic elements, to produce hydrides, carbides, nitrides, or oxides (Willmott *et al.*, 1994; Xiao *et al.*, 1996; Timm *et al.*, 1997; Verardi *et al.*, 1997; Willmott *et al.*, 1999b). The gas can be activated by using a low pressure RF discharge plasma source that provides a continuous flow of partially ionized gas, though problems can arise if the target itself reacts with this aggressive medium and its ablation properties change over time. When such a RF discharge source is not available, the reaction often requires relatively high background pressures. Above about 10 Pa, most of the initial kinetic and internal energy of the ablation plasma is quenched by multiple collisions with the ambient gas on its journey from target to substrate, obviating one of the most important benefits of PLD.

Wood *et al.* (1998), however, have utilized the quenching effect of a background gas at pressures of about 20 Pa to their advantage to produce nanoparticulates with a narrow range in size. Expansion of an ablation plume into an ambient background results in shock waves due to “ploughing” of the plume as it propagates through the gas (Wood *et al.*, 1997). Multiple collisions dissipate the kinetic energy of the ablation species until they slow sufficiently to nucleate and form nanoclusters in the shock fronts. The spatial and temporal brevity of these shock fronts ensures that the range of cluster sizes is small.

Compound targets are often employed in PLD, particularly in the production of dielectric and ceramic films and other multielemental oxides and nitrides (Kwon *et al.*, 1993; Verardi *et al.*, 1998). This is perhaps PLD’s greatest advantage over other deposition techniques, and has been most famously exploited in the thin-film growth of ceramic superconductors (Gross *et al.*, 1990; Kwon *et al.*, 1993). Congruent ablation is not always guaranteed, however, while preparation of compound targets represents its own set of problems. Sintering is an expensive and complicated process, and material densification is often critical in avoiding excessive out-

gassing and target exfoliation. Sample purity is rarely better than 1 part in 10 000. Noncongruent material transfer is sometimes compensated for by enriching one or more elemental components in the target, though, as the degree of congruent transfer also depends on experimental conditions, this approach is both empirical and unreliable. Reactive PLD and pulsed reactive crossed-beam laser ablation are preferred for “simple” chemical systems such as binary oxides, nitrides, carbides, and their solid solutions, especially when the highest purity is demanded.

### G. Femtosecond ablation

Today, femtosecond (fs) ablation is hailed as the state-of-the-art technique for optimal control of material removal. The advantage of using fs radiation<sup>1</sup> lies in (a) the ability to decouple the ablated volume from the adjoining target mass, and (b) the lowering of the threshold ablation fluence by a factor of  $10\text{--}10^2$  compared to ns work [see Eq. (2)]. This means that even the most intractable materials, such as the refractory metals, can be cleanly and congruently ablated. Laser droplet production is therefore much reduced.

When the laser pulse length  $\tau$  becomes shorter than the time needed to couple the electronic energy to the lattice, i.e., a few picoseconds, heat diffusion becomes insignificant and the dependence on  $\tau$  of the ablation threshold fluence becomes weaker than the  $\tau^{1/2}$  scaling described at the beginning of this section for longer pulse durations (Stuart *et al.*, 1995; Lenzner *et al.*, 1998). This thermal decoupling means that ablation occurs without collateral damage to the target. At least for nominally transparent dielectrics such as sapphire or silica, the penetration depth is much smaller than the normal absorption depth, as ablation is seeded by multiphoton ionization (MPI), followed by rapid Joule heating of these newly promoted conduction electrons by the laser radiation and further collisional (avalanche) ionization. The electronic energy is then deposited in the lattice within a few ps and, above threshold, this results in explosive material removal. Femtosecond ablation is therefore very efficient, and most of the input photonic energy can be accounted for by vaporization of the ablated volume and the degree of ionization and kinetic energies of the liberated species.

Multiphoton ionization is most efficient for low-bandgap materials or when using ultrashort pulses of less than 10 fs, whereas avalanche or electron collisional processes dominate for large bandgap materials. The efficiency of multiphoton ionization is also facilitated by the large Fourier-limited bandwidth of fs pulses, where  $\Delta\omega \approx 1/\Delta t$  is given by Heisenberg’s uncertainty principle, and can be as large as 30 nm for a femtosecond Ti:sapphire laser centered at 780 nm. Therefore the density and exact energetic positions of intragap states need

not be high and precise, respectively, for resonance-enhanced MPI (REMPI) to play a significant role. Similarly, repeated irradiation of the same volume at a fluence that is too low to produce ablation for the first pulse, can gradually disrupt the crystal structure so that ablation begins to occur once the defect density becomes sufficiently high (Campbell *et al.*, 1998).

Material damage is expected when the electron energy density is equal to the lattice binding energy per unit volume  $E_B$ , i.e.,  $\Delta E_g \cdot n_e = \Delta E_B$ , where  $\Delta E_g$  is the bandgap energy. This occurs in the range of  $n_e = 10^{19}\text{--}10^{22}\text{ cm}^{-3}$  (Stuart *et al.*, 1995; Campbell *et al.*, 1998). Experimental verification of this model must be handled carefully, primarily due to the strong dependence of MPI on laser intensity. Lenzner *et al.* (1998) have recently performed fs ablation of fused silica using a spatially homogenized beam free from “hot spots,” and although confirming the model of Stuart *et al.*, they found the ablation threshold to be a factor of 2 higher.

Large ranges of kinetic energies have been reported, depending on the nature of the ablation target, in particular its bandgap. Hence fs ablation of sapphire at a fluence 1.5 times that of the damage threshold results in  $\text{Al}^+$  ions with kinetic energies up to 300 eV (Varel *et al.*, 1998), while for GaAs, fs ablation at very low fluences occurs efficiently via Joule heating and avalanche ionization alone and produces species with kinetic energies of between 0.1 and 0.5 eV (Cavalleri *et al.*, 1998). Particularly high control of the kinetic energy is also expected for fs ablation of metals.

Despite its enormous promise, there has been very little work on film growth using fs PLD, probably because of its relative infancy. Nanosecond lasers continue to prevail in PLD due to their ease of handling and relative low cost. Notwithstanding many recent advances, fs PLD will remain within the province of well-funded research laboratories until fs lasers become easier to operate and fs pulse amplifiers become cheaper.

## III. PULSED REACTIVE CROSSED-BEAM LASER ABLATION

### A. Principal features

The combination of laser ablation and a pulsed secondary gas has long been known as a powerful tool for creating nonthermal species in cluster physics, for example in the discovery of the fullerenes (Kroto *et al.*, 1985). The ablated particles are entrained in a gas pulse confined to a narrow channel. Multiple collisions among the particles lead to the production of clusters, which then emerge in a supersonic jet from the channel exit (Powers *et al.*, 1982).

The first use of a pulsed gas in PLD was by Gupta and Hussey (1991) who used the reactive gas oxygen to make films of high- $T_c$  superconductors. As they pointed out, using a pulsed gas source enables one to limit the provision of reactive gas to the time period when transfer and deposition of ablated material occurs, which for repetition rates typically of 10 Hz and gas pulse dura-

<sup>1</sup>The term “femtosecond pulses” covers pulse lengths ranging from the shortest 6-fs pulse to approximately 200 fs.

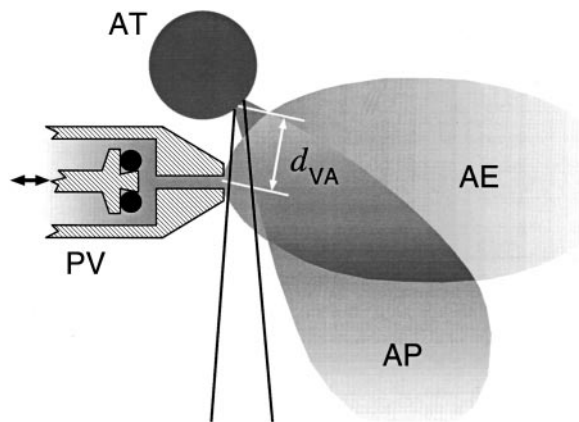


FIG. 3. Principal of pulsed reactive crossed-beam laser ablation. The labeling is as follows: PV=pulsed valve; AT=ablation target;  $d_{VA}$ =separation between PV nozzle exit and point of ablation, typically  $\leq 10$  mm; AE=adiabatic expansion; AP=ablation plume. Where the plume and pulsed gas cross is called the interaction region.

tions of a few hundred microseconds, implies a duty cycle of  $10^{-3}$ . This enormously reduces gas consumption, thereby allowing the possibility of *in-situ* analytical techniques, such as reflection high-energy electron-diffraction (RHEED) (Willmott *et al.*, 1998).

The essential difference between the experimental setup used by Gupta and Hussey, and that used by us lies in the distance  $d_{VA}$  between the ablation laser focus and the pulsed valve nozzle (see Fig. 3). By keeping this less than approximately 10 mm (see below), it is possible, via collisions in the interaction region where the two beams cross and where their number densities are  $\sim 10^{15} \text{ cm}^{-3}$ , to couple some of the internal and kinetic energy of the ablation plume species to the gas pulse. Thereafter, both the plasma and gas pulse expand further into vacuum and become collisionless. In our setup, opening a valve with a 2 bar stagnation pressure for  $\approx 400 \mu\text{s}$  generates adiabatically cooled pulses containing  $\sim 10^{17}$  particles having temperatures of  $\sim 20$  K. It is the initial collisions and the subsequent free expansion that provide and maintain the reactivity for enhanced film growth.

In our first experiments using pulsed reactive crossed-beam laser ablation, we grew CuO by ablating Cu metal and crossing the plume with an  $\text{N}_2\text{O}$  pulsed expansion. We established that processes occurring in the interaction region are essential for growth of high quality films at low temperature (Willmott *et al.*, 1994).

If the delay between the gas pulse trigger and laser pulse trigger was set within  $\pm 100 \mu\text{s}$  of the optimal value, for which the densest portions of both the plasma and gas pulse crossed, single-phase CuO thin films were produced on a MgO substrate placed 60 mm downstream from the pulsed valve. All other delays resulted in predominantly Cu films with some  $\text{Cu}_2\text{O}$  included. In a further experiment, the optimal delay was used but the point of ablation on the target was raised 7 mm above the axis of the pulsed valve (i.e., out of the plane of the paper in Fig. 3). This was enough to more than double

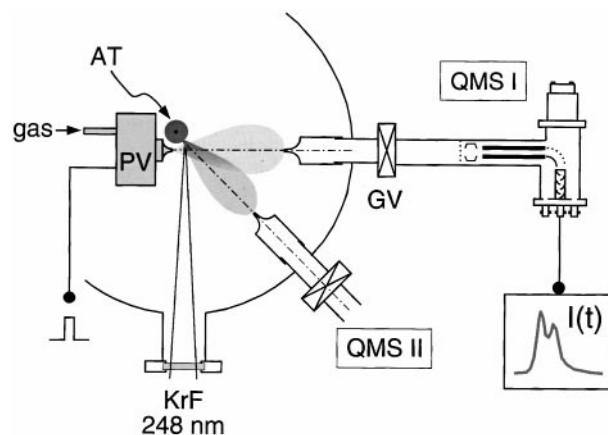


FIG. 4. Schematic of the dual time-of-flight quadrupole mass spectroscopy apparatus used to investigate scattering processes between an ablation plasma and free gas expansion. The labeling is as follows: AT=ablation target; PV=piezoelectric pulsed valve; GV=gate valve. The plasma is crossed with a gas pulse. For reasons of clarity, only QMS I is shown. The mass filtered species are deflected to a secondary electron multiplier by deflection plates [adapted from Willmott *et al.* (1997)].

the distance between the two beams' respective points of origin, and so reduce the number of collisions by effectively shifting the interaction region further downstream where the number density was estimated to be more than an order of magnitude lower. On the other hand, it had only an insignificant effect on the positions of the laser plume and gas pulse relative to the substrate. If the film chemistry merely depended on the Cu plasma and  $\text{N}_2\text{O}$  pulse arriving simultaneously at the substrate surface, this small vertical shift in the ablation focus spot would not have been expected to substantially affect the film properties. We discovered, however, that in this control experiment unoxidized Cu films were produced. This result proved that scattering processes between the pulsed expansion and the laser plume are responsible for the enhanced reactivity in pulsed reactive crossed-beam laser ablation.

In the following, we summarize the scattering processes in the interaction region between the ablation plume and the pulsed gas expansion, then discuss the effect of this on the growth of thin films.

## B. Reactive scattering processes

The experimental setup used to investigate scattering processes between an ablation plasma and a gas pulse expansion is shown in Fig. 4 (Willmott *et al.*, 1997).

The visual effect of crossing a pulsed expansion with an expanding ablation plasma is dramatic (see Fig. 5). Luminescence from the plasma becomes greater, the color may change somewhat, and the visible extent of the plasma changes, usually becoming larger. All this is true if the laser trigger delay relative to the gas pulse trigger has been "optimized." For inappropriate delays, the plasma expands into the residual background gas, typically of less than 0.1 Pa, caused by the finite pump-

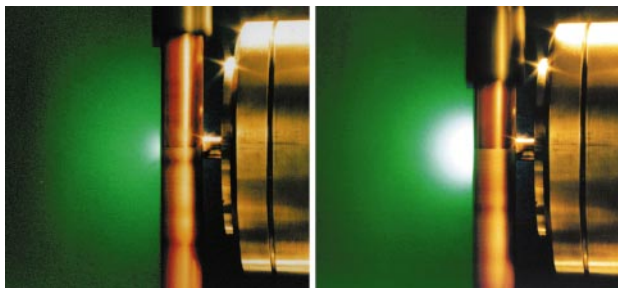


FIG. 5. Change in the visual appearance of a Cu ablation plume propagating into a vacuum (left image), and crossed with an  $N_2O$  gas pulse (right image) [Color].

ing speed of the vacuum system. The difference between expanding into vacuum and into this residual background is visually undetectable.

In all our TOFQMS experiments performed to date on the species resulting from crossing an ablation plume with a gas pulse, no associative products could be detected in the gas phase. Hence, for the Ti/ $N_2$  system, no TiN,  $Ti_2N$ , or Ti clusters were found. This is perhaps not surprising, as at these high collision energies, any associative product will be highly internally excited, and will fragment within a vibrational time period. Such processes may, however, contribute to the production of gas pulse molecule fragments via excited transition states. Only three-body collisions and electron ejection might allow stable associative products to occur, though Tang *et al.* (1976) have shown such processes to have several orders of magnitude smaller cross sections than the total scattering cross sections. Because the high-density gas pulse within the interaction region is so temporally and spatially localized, it rapidly becomes free to expand. This explains why we did not observe the cluster formation described by Wood *et al.* (1998).

The collision rate  $Z_P$  of a plasma particle  $P$  moving at a velocity  $\bar{c}$  relative to a collection of gas pulse particles  $G$  having a number density  $N_G$  is given by

$$Z_P = \pi d^2 \bar{c} N_G, \quad (7)$$

where  $d$  is the collision parameter between  $P$  and  $G$  and is of the order of 1.5 Å, while  $\bar{c}$  may be several kilometers per second. The number density distribution in a supersonic expansion is a function of angle, distance from the exit nozzle, and time, and has been well described by Scoles (Scoles, 1988). For a typical pulse containing  $n_{\text{pulse}} = 10^{17}$  particles and having a pulse length of  $\tau_{\text{pulse}} = 400 \mu\text{s}$ , the peak pressure at 1 cm from the exit nozzle (where the ablation particle traverses the gas pulse) is about  $10^2$  Pa and its lateral extent is also of the order of 1 cm.  $Z_P$  is therefore about  $10^7 \text{ s}^{-1}$ , and  $P$  will therefore suffer approximately 10 collisions on its path through the gas pulse. At 0.1 Pa, however, the same particle has a mean free path well in excess of the vacuum chamber dimensions.

The effect of the ablation plume on the gas pulse as the former propagates through the latter is shown in Fig. 6 for a Ti ablation plume and an  $N_2$  gas pulse. Under typical conditions, the integrated time-of-flight signal is

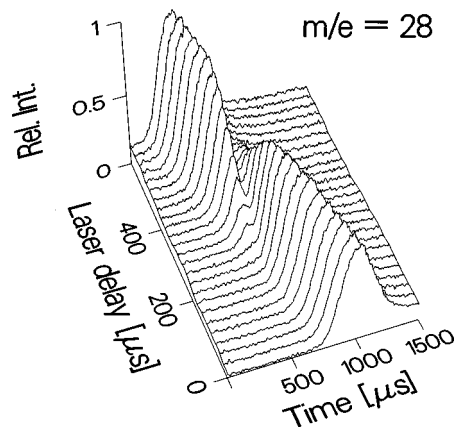


FIG. 6. Time-of-flight signal for the  $N_2$  gas pulse as a function of laser delay. Data acquisition is triggered from the laser trigger, hence the pulse peak also shifts for each step by the change in laser delay (here, 25  $\mu\text{s}$ ). Note the depletion caused by scattering with the ablation plasma for delays centered at 375  $\mu\text{s}$ . From Willmott *et al.* (1997).

depleted by some 10%, which agrees fairly well with  $10^{15}$  ablation particles, each deflecting 10 gas particles from their original direction. The ablation pulse as it passes through the gas pulse has a temporal width of about  $\tau_{\text{plasma}} \sim 10 \mu\text{s}$ , and will therefore sample a section of the gas pulse containing about  $n_{\text{pulse}} \cdot \tau_{\text{plasma}} / \tau_{\text{pulse}}$  particles. For the typical values given above, this equates to some  $5 \times 10^{15}$  gas particles. As this is only approximately 5 times the number of particles in the ablation plume, and considering the collision frequency  $Z_P \sim 10$ , it can be expected that the pulsed gas, or “collision medium,” will become so depleted that considerable bleaching in the interaction volume is expected, and the scattering process will deviate from a linear Lambert-Beer formalism. We indeed find that the fractional depletion depends on  $n_{\text{pulse}}$ .

Fast N atoms and  $N^+$  ions are also produced in the interaction region. Inelastic collisions between molecules may result in ionization of one or both colliding partners (Massey and Gilbody, 1974). Because the plasma species are more than an order of magnitude faster than the molecules emerging from the pulsed valve, we approximate the latter as being stationary. For a head-on collision between a particle  $m_1$  traveling at a velocity  $v_i$  and a stationary particle  $m_2$ , the maximum fraction of kinetic energy that can be transferred from the first particle into internal energy of either collision partner is given by

$$\frac{\Delta U}{U} = \frac{m_2}{m_1 + m_2}, \quad (8)$$

which, for Ti and  $N_2$ , leads to a 23% maximal energy transfer for each collision.

The first ionization potential of most metals lie between 6 and 8 eV, well below the typical kinetic energies of the ablation species of the order of 30 eV, hence even ground-state metal atoms from the plume can be readily ionized by colliding with a gas particle. This is shown

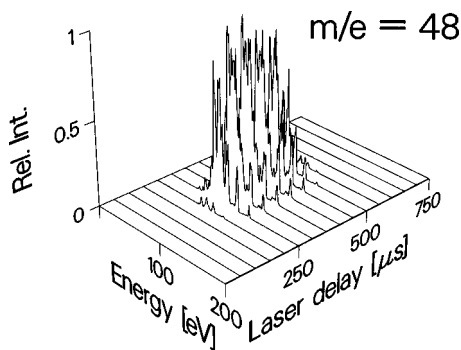


FIG. 7. The translational energy distribution  $P(E_i)$  of  $\text{Ti}^+$  ions ( $m/e=48$ ) as a function of laser trigger delay after the gas pulse trigger. From Willmott *et al.* (1997).

clearly in Fig. 7 for  $\text{Ti}^+$  as a function of laser delay with the  $\text{N}_2$  expansion. The ion signal increases by over two orders of magnitude for laser delays around the optimum value. This cannot be explained by simple elastic scattering for two reasons. One might consider the increase in signal in the QMS I direction (see Fig. 4) to be due to entrainment of  $\text{Ti}^+$  ions in the  $\text{N}_2$  gas. This would require considerable momentum transfer from the slow  $\text{N}_2$  molecules to the rapid Ti species in the direction of the pulsed gas axis, which for the collisional frequencies calculated above appears to be impossible. If this were nonetheless the case, such a process would require a concomitant depletion of signal in the QMS II direction as the  $\text{Ti}^+$  ions are swept away. However, just the opposite is found. It is therefore apparent that the increased  $\text{Ti}^+$  signal is produced as a result of inelastic scattering of the Ti plasma with the  $\text{N}_2$  pulse. Langmuir probe measurements also show the same increase and allow us to obtain a rough value for the absolute degree of ionization, which is found to be  $\sim 10^{-3}$  and  $0.28 \pm 0.11$  for the ablation plume propagating into vacuum and through the gas pulse, respectively (Willmott *et al.*, 1997). We have found similar data for other systems, for example with an Si plasma and  $\text{N}_2$  pulse, for which the increase in ion signal is less pronounced than for Ti and  $\text{N}_2$ , presumably because of the higher first ionization potential of Si of 8.2 eV (Spillmann and Willmott, 1999).

Because the collision velocity  $v_i$  is so much smaller than classical orbital electron velocities, it is possible that the precise mechanism for collision-induced ionization at these kinetic energies takes place through excitation of two electrons (Weizel, 1932). This excited complex state might have sufficient internal energy that under rearrangement, one electron is liberated into the continuum in a manner similar to the production of Auger electrons. Indeed, we see signal at  $m/e=24$  for both the neutral and ionic species, which implies a significant fraction of the Ti species are already  $\text{Ti}^{2+}$  ions in the plasma and that double ionization of excited neutrals by the QMS ionizer head is relatively efficient. Hence energy transfer proceeds first via the relatively efficient process of collisions between molecules or atoms of similar mass, which is then converted to ejection of an electron by electronic rearrangement.

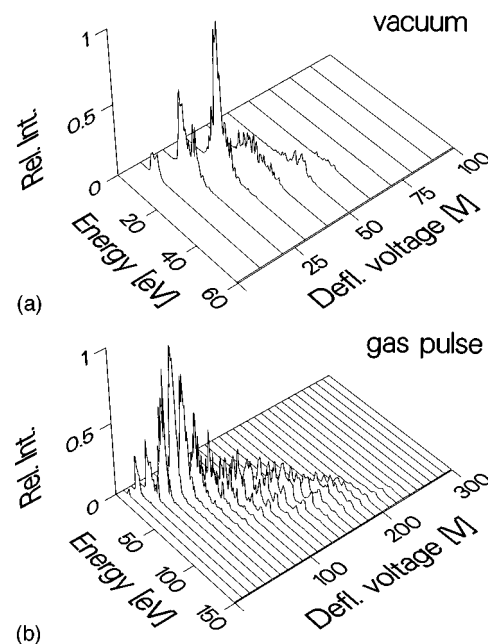


FIG. 8. The translational energy distribution  $P(E_i)$  of  $\text{Ti}^+$  ions as a function of deflection voltage  $V_{\text{defl}}$  for expansion into vacuum with no gas pulse (upper trace) and at the optimum laser delay of  $\delta t=375 \mu\text{s}$  and an  $\text{N}_2$  backing pressure of 2 bars (lower trace). Note the different energy and voltage scales for the two plots. From Willmott *et al.* (1997).

The kinetic energy distributions produced by Jacobean transformations of the time-of-flight data (also accounting for the dependence of detection sensitivity on particle velocity) as a function of the deflection voltage  $V_{\text{defl}}$  are shown in Fig. 8 for  $\text{Ti}^+$  ions propagating into vacuum and crossing an  $\text{N}_2$  pulse.  $V_{\text{defl}}$  deflects the ions onto the secondary electron multiplier and so acts as an energy filter for the ions. The majority of ions have energies in the region of 20–30 eV, but a tail extends to above 100 eV when the plasma is crossed with the gas pulse. This slight increase in average kinetic energy and spread to higher energies may in part be due to an increased cross section for collision-induced ionization with relative velocity (Massey and Gilbody, 1974; Tang *et al.*, 1976).

The interaction region therefore attains a high degree of ionization within about a microsecond as the plasma passes through the gas pulse. From this moment on we develop a model of the evolution of the plasma. We approximate the interaction region as a plasma sphere of radius  $R$  which initially contains  $n_i=n_e$  ions and electrons. The electrons, because of their approximately 300 times higher velocity, escape more rapidly from the plasma. The most energetic electrons escape first, leaving behind a plasma with a Maxwell-Boltzmann energy distribution of its electrons up to the electrostatic potential at the plasma surface, and zero above this energy, as these electrons have escaped to infinity, which in effect means they have been conducted away at the chamber walls (Dreyfus, 1991). We are now faced with a problem of self-consistency. As more electrons leave, the surface electrostatic potential rises as the net positive charge left

within the plasma increases. Eventually, the surface potential is just enough to stop all the remaining electrons from escaping to infinity, i.e., the most energetic electrons remaining within the influence of the plasma have a kinetic energy equal to the surface electrostatic potential.

The fraction of electrons with energies greater than  $\mathcal{E}_0$  is given by

$$\int_{x_0}^{\infty} \frac{2}{\sqrt{\pi}} x^{1/2} e^{-x} dx, \quad (9)$$

where  $x = \mathcal{E}/kT_e$ . For  $x_0 = \mathcal{E}_0/kT_e \gg 1$ , this integral is approximately given by

$$\frac{2}{\sqrt{\pi}} x_0^{1/2} e^{-x_0}. \quad (10)$$

Hence the excess charge remaining in the plasma is given by

$$\frac{2}{\sqrt{\pi}} x_0^{1/2} e^{-x_0} n_e e, \quad (11)$$

where  $e$  is the electronic charge. The electrostatic potential felt by an electron at the surface of a sphere of radius  $R$  containing a charge  $Q$  is given by

$$V = \frac{Qe}{4\pi\epsilon_0 R} = \frac{2}{\sqrt{\pi}} \frac{x_0^{1/2} e^{-x_0} n_e e^2}{4\pi\epsilon_0 R}. \quad (12)$$

This we can set equal to the voltage equivalent of the electron temperature of the electrons with energy  $\mathcal{E}_0$  so that

$$\frac{2}{\sqrt{\pi}} \cdot \frac{x_0^{1/2} e^{-x_0} n_e e}{4\pi\epsilon_0 R} = kT_e \cdot x_0, \quad (13)$$

where we have expressed  $kT_e$  in electron volts. We therefore finally obtain

$$\frac{e^{-x_0}}{x_0^{1/2}} = \frac{\sqrt{\pi} kT_e (\text{in eV}) \cdot 4\pi\epsilon_0 R}{2n_e e}. \quad (14)$$

Inserting typical experimentally determined values found for the Ti/N<sub>2</sub> system, we obtain  $\mathcal{E}_0 = (22 \pm 1.3)$  eV, which is the potential of the plasma which will accelerate the positive ions towards ground and is achieved at the expense of electron energy. Once this surface potential has built up, we can consider its evolution on the time scale of the ions. We can now assume that the plasma charge remains unchanged, that is the ion flux is equal to the electron flux (Dreyfus, 1991), and the surface potential will develop to reduce the rate of electron escape to the natural rate of ion escape. The ions that most readily escape are those that are causing the surface potential barrier for the electrons, hence the surface ions are being slowly replaced by lower energetic ions as the former escape, and the potential drops.

The rate of escape  $dn_i/dt$  of ions from the interaction region of volume  $V_{\text{int}}$  and area  $A_{\text{int}}$ , is given by

$$\frac{dn_i}{dt} = \frac{n_i A_{\text{int}} \bar{v}}{4V_{\text{int}}}, \quad (15)$$

where  $\bar{v} = (2/\sqrt{\pi})(2kT_i/m)^{1/2}$  is the mean velocity. For a plasma sphere initially of 7 mm radius and having an ion temperature of 10 000 K ( $kT_i \sim 1$  eV), the rate of escape is therefore approximately  $1.6 \times 10^{20}$  ions per second, and the interaction volume will be entirely extinguished after some 3  $\mu\text{s}$ .

This model explains the increase in ion energies as a result of crossing the ablation plasma with a gas pulse. The initial kinetic energy of the ablation species is partially consumed in fragmentation of gas pulse molecules and ionization of both ablation and gas pulse atoms. At the plasma temperatures under consideration, many of the ablation neutrals will have already been in an excited electronic state before they ionize through collisions with the N<sub>2</sub> molecules. The sudden increase in the degree of ionization leads to a renewed acceleration of the positive ions, which results in kinetic energies larger than those obtained in vacuum. The extra energy is accounted for by the initial electronic excitation. This explains the accompanying increase in the modal kinetic energy of Ti<sup>+</sup> after interaction with the gas pulse, shown in Fig. 8, though, as mentioned above, the high energy tail may also be partly due to the increased efficiency of collision induced ionization with relative collisional velocity.

In summary, the reactive scattering processes that occur in the dense region where the ablation plasma crosses with the gas pulse allow some of the internal energy of the ablation plume not only to be redistributed within the plasma itself, but also to be coupled to the gas pulse species to form activated species. These, by virtue of the pulsed nature of both beams, can further propagate under quasicollisionless conditions and thereby preserve their reactivity, until they reach the substrate, where associative reactions occur to produce the thin films. The chemistry is hence less determined by the substrate temperature than by the nonthermal processes occurring in the gas phase, which allow reactions to occur far from chemical equilibrium.

This fundamental aspect of pulsed reactive crossed-beam laser ablation has been clearly demonstrated by contrasting our success in growing GaN using Ga ablation with an N<sub>2</sub> pulse (Willmott and Antoni, 1998) with the results of Xiao *et al.* (1996), who were unable to grow GaN by Ga ablation in 1 mbar of N<sub>2</sub> background gas.

Pulsed reactive crossed-beam laser ablation lends itself particularly to the thin film growth of materials for which one subset of elemental components is supplied by ablation of high purity elements or alloys (mainly metals), and a second subset in the form of a gas. In this manner, simple oxides [CuO, (Willmott *et al.*, 1994), Ti-doped sapphire (Willmott *et al.*, 1999b)], nitrides [TiN (Willmott *et al.*, 1997), GaN (Willmott and Antoni, 1998)], carbides [SiC (Spillmann and Willmott, 1999)],

TABLE I. Materials used and films grown using pulsed reactive crossed-beam laser ablation.

Ablation target	Gas	Film	Substrate
Cu	N <sub>2</sub> O	CuO(111)	MgO(001)
Ti	N <sub>2</sub> /CH <sub>4</sub>	TiC <sub>x</sub> N <sub>y</sub> (001)	Si(001)
Ga	N <sub>2</sub>	GaN(001), GaN(111)	Si(001), Si(111)
Ga-Al alloy	N <sub>2</sub>	Al <sub>x</sub> Ga <sub>1-x</sub> N(111)	Si(111)
Ti:Al (0.002:0.998)	O <sub>2</sub>	Ti:Al <sub>2</sub> O <sub>3</sub> (0001)	Al <sub>2</sub> O <sub>3</sub> (0001)
Zr	N <sub>2</sub> /CH <sub>4</sub>	ZrC <sub>x</sub> N <sub>y</sub> (001)	Si(001)
C	N <sub>2</sub> /NH <sub>3</sub>	<i>a</i> -CN <sub>x</sub>	Si(001)
Si	N <sub>2</sub> , CH <sub>4</sub>	<i>a</i> -SiN <sub>x</sub> , SiC(001)	Si(001)
YBa <sub>2</sub> Cu <sub>3</sub> O <sub>7-x</sub>	O <sub>2</sub> /N <sub>2</sub> O	YBa <sub>2</sub> Cu <sub>3</sub> O <sub>7-x</sub> (001)	SrTiO <sub>3</sub> (001)

and solid solutions of these can thus be fabricated using pulsed reactive crossed-beam laser ablation, although it has also successfully been used for the epitaxial growth of YBa<sub>2</sub>Cu<sub>3</sub>O<sub>7-x</sub> on SrTiO<sub>3</sub>. A list of materials used for both subsets, and films grown using this technique is given in Table I.

#### IV. CONCLUDING REMARKS

If one were to set out the properties of the ideal deposition method for a broad set of materials, PLD would stand out as perhaps the most promising choice from the selection available today: faithful congruent transfer from bulk to film is possible; the energy range of the impinging particles is exactly that needed to promote surface diffusion while avoiding bulk damage; the species are often activated, either as ions or electronically excited neutrals, which facilitate associative chemistry on the growing film; and, especially for sub-ns radiation, virtually all materials can be ablated. There remain, however, some technological obstacles which still need to be overcome. By far the most important of these are laser droplet production and impurity levels. The first of these problems seems to be partially resolved for bulk targets that can be melted, though using fs lasers appears to be a more universal solution, although the equipment is presently very expensive and user unfriendly. Pulsed reactive crossed-beam laser ablation also provides a solution as lower laser fluences are generally required, due to the improved reactivity caused by crossing the ablation plume with a gas expansion. At least for simple chemical systems, it can also overcome problems of impurities, by using easily available high purity metallic elemental and alloy ablation targets and high-purity gases.

PLD has already found a commercial niche for growing devices such as Josephson junctions made from cuprate superconductors (Gross *et al.*, 1990). Its application seems imminent for hard coatings such as carbides, nitrides, and borides, in which adhesion of the layer to the substrate can be improved by high-energy bombardment and the need for perfect crystal perfection is relaxed. The most stringent demands lie in the field of semiconductor technology (Chern *et al.*, 1995), and it is hoped that PLD and pulsed reactive crossed-beam laser

ablation, in conjunction with fs ablation, become established as key tools for scientists and engineers striving to integrate ever more differing and numerous materials in a single device, thereby realizing the potential of these elegant methods.

#### ACKNOWLEDGMENTS

The authors gratefully acknowledge financial support by the Schweizerische Nationalfonds zur Förderung der wissenschaftlichen Forschung. Special thanks go to Roman Timm, Frederic Antoni, Periasamy Manoravi, and Hannes Spillmann for their invaluable contributions to the success of this work.

#### REFERENCES

- Archbold, E., D. W. Harper, and T. P. Hughes, 1964, *Br. J. Appl. Phys.* **15**, 1321.
- Brice, D. K., J. Y. Tsao, and S. T. Picraux, 1989, *Nucl. Instrum. Methods Phys. Res. B* **44**, 68.
- Bunshah, R. F., 1994, *Handbook of Deposition Technologies for Films and Coatings* (Noyes, Park Ridge, NJ).
- Burger, W. R., and R. Reif, 1987, *J. Appl. Phys.* **62**, 4255.
- Campbell, E. E. B., D. Ashkenasi, and A. Rosenfeld, 1998, in *Lasers in Materials*, edited by R. P. Agarwala (Trans-Tech, Zürich, Switzerland), p. 123.
- Cavalleri, A., K. Sokolowski-Tinten, J. Bialkowski, and D. von der Linde, 1998, *Appl. Phys. Lett.* **72**, 2385.
- Chang, J. J., and B. E. Warner, 1996, *Appl. Phys. Lett.* **69**, 473.
- Chapman, B., 1980, *Glow Discharge Processes* (Wiley, New York).
- Chen, F. F., 1974, in *Plasma Diagnostic Techniques*, edited by R. H. Huddlestone and S. L. Leonard (Academic, London, England), p. 1.
- Chern, M. Y., H. M. Lin, C. C. Fang, J. C. Fan, and Y. F. Chen, 1995, *Appl. Phys. Lett.* **67**, 1390.
- Chrisey, D. B., and G. K. Hubler, 1994, Eds., *Pulsed Laser Deposition of Thin Films* (Wiley, New York).
- Curl, R. F., and R. E. Smalley, 1991, *Sci. Am.* **265**, 32.
- Dreyfus, R. W., 1991, *J. Appl. Phys.* **69**, 1721.
- Friichtenicht, J. F., 1973, *Rev. Sci. Instrum.* **45**, 51.
- Geohegan, D. B., 1992, in *Laser Ablation of Electronic Materials: Mechanisms and Applications*, edited by E. Fogarassy and S. Lazare (North-Holland, Amsterdam), p. 73.

- Geohegan, D. B., 1993, in *Laser Ablation in Materials Processing: Fundamentals and Applications*, edited by B. Braren, J. J. Dubowski, and D. P. Norton, MRS Symposia Proceedings No. 285 (Materials Research Society, Pittsburgh), p. 27.
- Gross, R., P. Chaudhari, M. Kawasaki, M. B. Ketchen, and A. Gupta, 1990, *Appl. Phys. Lett.* **57**, 727.
- Gupta, A., and B. W. Hussey, 1991, *Appl. Phys. Lett.* **58**, 1211.
- Hansen, T. N., J. Schou, and J. G. Lunney, 1997, *Europhys. Lett.* **40**, 441.
- Hendron, J. M., R. A. Al-Wazzan, C. Mahony, T. Morrow, and W. G. Graham, 1996, *Appl. Surf. Sci.* **96–98**, 112.
- Hirvonen, J. K., 1991, *Mater. Sci. Rep.* **6**, 215.
- Hubler, G. K., 1994, in *Pulsed Laser Deposition of Thin Films*, edited by D. B. Chrisey and G. K. Hubler (Wiley, New York), p. 327.
- Hughes, T. P., 1975, *Plasmas and Laser Light* (Wiley, New York).
- Kelly, R., and A. Miotello, 1993, *Appl. Phys. B: Photophys. Laser Chem.* **57**, 145.
- Kelly, R., A. Miotello, B. Braren, A. Gupta, and K. Casey, 1992, *Nucl. Instrum. Methods Phys. Res. B* **65**, 187.
- Kroto, H. W., J. R. Heath, S. C. O'Brien, R. F. Curl, and R. E. Smalley, 1985, *Nature (London)* **318**, 162.
- Kwon, C., *et al.*, 1993, *Appl. Phys. Lett.* **62**, 1289.
- Lenzner, M., J. Krüger, S. Sartania, Z. Cheng, Ch. Spielmann, G. Mourou, W. Kautek, and F. Krausz, 1998, *Phys. Rev. Lett.* **80**, 4076.
- Lewis, B., and J. C. Anderson, 1978, *Nucleation and Growth of Thin Films* (Academic, London, England).
- Massey, H. S. W., and H. B. Gilbody, 1974, *Electronic and Ionic Impact Phenomena*, Vol. 4, (Oxford University, London).
- Murray, P. T., and D. T. Peeler, 1993, *Appl. Surf. Sci.* **69**, 225.
- Nagai, I., T. Tagathaki, A. Ishitani, H. Kuroda, and M. Yoshikawa, 1988, *J. Appl. Phys.* **64**, 5183.
- Nakamura, S., N. Isawa, M. Senoh, and T. Mukai, 1992, *Jpn. J. Appl. Phys., Part 1* **31**, 1258.
- Park, S. M., and J. Y. Moon, 1998, *J. Chem. Phys.* **109**, 8124.
- Powers, D. E., S. G. Hansen, M. E. Geusic, A. C. Pulu, J. B. Hopkins, T. G. Dietz, M. A. Duncan, P. R. R. Langridge-Smith, and R. E. Smalley, 1982, *J. Phys. Chem.* **86**, 2556.
- Ready, J. F., 1963, *Appl. Phys. Lett.* **3**, 11.
- Ready, J. F., 1978, *Industrial Applications of Lasers* (Academic, New York).
- Russo, R. E., 1995, *Appl. Spectrosc.* **49**, 14A.
- Saenger, K. L., 1994, in *Pulsed Laser Deposition of Thin Films*, edited by D. B. Chrisey and G. K. Hubler (Wiley, New York), p. 581.
- Sankur, H., W. J. Gunning, J. DeNatale, and J. F. Flintoff, 1989, *J. Appl. Phys.* **65**, 2475.
- Schey, B., T. Bollmeier, M. Kuhn, W. Biegel, and B. Stritzker, 1998, *Rev. Sci. Instrum.* **69**, 474.
- Scoles, G., 1988, *Atomic and Molecular Beam Methods*, Vol. 1 (Oxford University, New York).
- Segall, S. B., and D. W. Koopman, 1973, *Phys. Fluids* **16**, 1149.
- Sibold, D., and H. M. Urbassek, 1992, *Phys. Fluids A* **4**, 165.
- Spillmann, H., and P. R. Willmott, 1999, *Appl. Phys. A* (in press).
- Stuart, B. C., M. D. Feit, A. M. Rubenchik, B. W. Shore, and M. D. Perry, 1995, *Phys. Rev. Lett.* **74**, 2248.
- Svensen, W., O. Ellegaard, and J. Schou, 1996, *Appl. Phys. A: Mater. Sci. Process.* **63A**, 247.
- Tang, S. P., N. G. Utterback, and J. F. Friichtenicht, 1976, *J. Chem. Phys.* **64**, 3833.
- Timm, R., P. R. Willmott, and J. R. Huber, 1996, *J. Appl. Phys.* **80**, 1794.
- Timm, R., P. R. Willmott, and J. R. Huber, 1997, *Appl. Phys. Lett.* **71**, 1966.
- van Ingen, R. P., 1996, *J. Appl. Phys.* **79**, 467.
- Varel, H., M. Wähmer, A. Rosenfeld, D. Ashkenasi, and E. E. B. Campbell, 1998, *Appl. Surf. Sci.* **127–129**, 128.
- Venables, J. A., G. D. T. Miller, and M. Hanbücken, 1984, *Rep. Prog. Phys.* **47**, 399.
- Verardi, P., M. Dinescu, F. Craciun, and A. Perrone, 1998, *Appl. Surf. Sci.* **127–129**, 457.
- Verardi, P., M. Dinescu, C. Gerardi, L. Mirengi, and V. Sandu, 1997, *Appl. Surf. Sci.* **109–110**, 371.
- von Engel, A., 1965, *Ionized Gases* (Clarendon, Oxford, England).
- Weaver, I., 1996, *J. Appl. Phys.* **79**, 7216.
- Weizel, W., 1932, *Z. Phys.* **76**, 250.
- Wiedeman, L., and H. Helvajian, 1991, *J. Appl. Phys.* **70**, 4513.
- Willmott, P. R., and F. Antoni, 1998, *Appl. Phys. Lett.* **73**, 1394.
- Willmott, P. R., P. Manoravi, and K. Holliday, 1999a, *Appl. Phys. A* (in press).
- Willmott, P. R., P. Manoravi, J. R. Huber, T. Greber, K. Holliday, and T. Murray, 1999b, *Opt. Lett.* **24**, 1581.
- Willmott, P. R., R. Timm, P. Felder, and J. R. Huber, 1994, *J. Appl. Phys.* **76**, 2657.
- Willmott, P. R., R. Timm, and J. R. Huber, 1997, *J. Appl. Phys.* **82**, 2082.
- Willmott, P. R., R. Timm, and J. R. Huber, 1998, *Appl. Surf. Sci.* **127–129**, 105.
- Wood, R. F., K. R. Chen, J. N. Leboeuf, A. A. Puretsky, and D. B. Geohegan, 1997, *Phys. Rev. Lett.* **79**, 1571.
- Wood, R. F., J. N. Leboeuf, K. R. Chen, D. B. Geohegan, and A. A. Puretsky, 1998, *Appl. Surf. Sci.* **127–129**, 151.
- Xiao, R. F., H. B. Liao, N. Cue, X. W. Sun, and H. S. Kwok, 1996, *J. Appl. Phys.* **80**, 4226.